Journal of
Composites Science

MDPI

Article

Electromagnetic Interference Shielding Effectiveness of Natural and Chlorobutyl Rubber Blend Nanocomposite

Tomy Muringayil Joseph [1], Hanna J. Mariya [2], Jozef T. Haponiuk [1,*], Sabu Thomas [2,*], Amin Esmaeili [3] and S. Mohammad Sajadi [4]

[1] Department of Polymer Technology, Faculty of Chemistry, Gdańsk University of Technology, G. Narutowicza 11/12, 80-233 Gdańsk, Poland
[2] School of Chemical Sciences, Mahatma Gandhi University, Kottayam 68660, Kerala, India
[3] Department of Chemical Engineering, School of Engineering, Technology and Industrial Trades, The University of Doha for Science and Technology (UDST), Arab League St., Doha 24449, Qatar
[4] Department of Nutrition, Cihan University-Erbil, Kurdistan Region, Erbil P.O. Box 624, Iraq
* Correspondence: jozef.haponiuk@pg.edu.pl (J.T.H.); sabuthomas@mgu.ac.in (S.T.); Tel.: +48-583472134 (J.T.H.)

Abstract: The science and technology of electrical equipment for communication experience a rapid growth rate. However, the unwanted interference of electromagnetic waves of different electronic devices brought serious anxiety about human health as well as the lifetime and performance of the systems. To combat these consequences, we need to lessen the electromagnetic wave emission by making our devices more noise-sensitive. Herein, we incorporated carbon nanotubes (CNTs) at different ratios into natural rubber (NR) and chlorobutyl rubber (CIIR) to achieve shielding efficiency, along with carbon nanofibers (CNFs), nanoclay (NC), and carbon black (CB) to manipulate EMI shielding performance. The blend of CIIR/NR in a 70/30 (*w*/*w*) ratio also mixed with CNT, CNF, CB and NC. The effect of different fillers and their concentration/combination was analyzed by UV spectroscopy, demonstrating an absorbance peak in CIIR in 320 nm. From FTIR spectroscopy, it was evident that CIIR/CNT (5 phr), NR (30 wt.%)/CIIR (70 wt.%)/CB (5 phr), and NR (30 wt.%)/CIIR (70 wt.%)/CNT (5 phr) new bonding signatures were detected. The dielectric spectroscopic analyses were reflected in dielectric loss, dielectric permittivity and AC conductivity, where NR (30 wt.%)/CIIR (70 wt.%)/CB (5 phr) blend nanocomposite with 5 dB showed significantly higher EMI shielding performance compared to CIIR/CNT (5 phr) and CIIR/CNF (5 phr) with 29 and 15 dB, respectively. The greater the concentration of nanofiller, the lower the electromagnetic interference (EMI) shielding, i.e., CIIR/CNT (10 phr) with 15 dB (≈−48% dB), but with more agglomeration. Surprisingly, even a combination of fillers did not lead to higher EMI performance, such that CIIR/CNT (5 phr)-CB (20 phr) showed an EMI shielding value of 59 dB.

Keywords: natural rubber; chlorobutyl rubber; nanocomposite; carbon nanotube; electromagnetic interference shielding

Citation: Muringayil Joseph, T.; Mariya, H.J.; Haponiuk, J.T.; Thomas, S.; Esmaeili, A.; Sajadi, S.M. Electromagnetic Interference Shielding Effectiveness of Natural and Chlorobutyl Rubber Blend Nanocomposite. *J. Compos. Sci.* **2022**, *6*, 240. https://doi.org/10.3390/jcs6080240

Academic Editor: Francesco Tornabene

Received: 17 May 2022
Accepted: 4 August 2022
Published: 15 August 2022

1. Introduction

The ever-increasing growth of electrical and electronic devices that are emitting electromagnetic energy, more or less in the same frequency bands, increases the concerns about the health of human beings adjacent to those devices as well as decreases the service life of those devices [1–3]. Such a disadvantage is called electromagnetic interference (EMI), which is an electrical phenomenon, arising from unwanted electromagnetic emission, either radiated or conducted. Since polymers are widely used for housing electronic devices, because of their light weight, flexibility in processing and manufacturing processes, and reasonable price, a great deal of attention has been paid to combat their EMI consequence [4,5]. Typically, making polymers conductive or using electrically conductive polymer composites has been known as a solution to their EMI pollution. On the other hand, EMI systems require high loadings of conventional fillers, which disrupts dispersion and consequently other

characteristics, such as mechanical strength [6,7]. Electromagnetic shielding (EMS) is the practice of reducing the electromagnetic field in a space by blocking the field with barriers made of conductive or magnetic materials. Commonly, polymers, elastomers, and plastics are electrically insulating and transparent to electromagnetic radiation; i.e., their EMI shielding effectiveness (SE) is equal to zero. However, both conductivity and EMI shielding effectiveness have been reported to be improved by the incorporation of conventional electrically conductive fillers such as conductive carbon black, carbon fiber, nickel-coated graphite fiber, and metal powders [8,9]. Indeed, each filler offers a set of advantages and disadvantages. Therefore, several other aspects of the conventional fillers such as anti-corrosion resistance, healing, and shape memory have been occasionally reported besides EMI performance [10–12]. Notably, engineering polymers used in electronics are also prone to difficult processing, particularly when conductive additives are incorporated [13,14]. Thus, tailoring shielding response of conductive polymer nanocomposites necessitates the careful selection of polymer and filler, along with using small-scale fillers with superior properties at lower loading levels to avoid EMI hazard [13,15,16].

Various carbonaceous fillers, such as Carbon nanotubes (CNTs), have piqued interest in conducting polymer nanocomposites that are capable of dissipating electrostatic charges and shielding devices from electromagnetic radiation, because of their low density, relatively small loading, large specific surface, and high intrinsic electrical conductivity combined with their very high aspect ratio. Refs. [17,18] Fabrication and characterization of conductive CNT/polymer nanocomposites have gained significant attention in recent years. Electro-magnetic interference (EMI) shielding and electrostatic dissipation (EDS) are two key uses of conductive polymer nanocomposites, both of which require modest conductivities for EMI [18,19]. The use of electronic technology and telecommunication gadgets has skyrocketed in recent years. Such electronic equipment creates EMI and radio frequency interference (RFI), which can cause an electrical disturbance that leads to performance failure. Electronic equipment EM radiation can cause interference with the source device and surrounding devices, resulting in negative consequences [20]. In recent years, numerous methodologies for analyzing EMI shielding of rubber matrices with various fillers have been performed. Despite this, limited research on the use of carbon fibers [21] and other nanoparticles filled with rubber to reduce electromagnetic radiation has been reported. [22,23]. Joseph et al. examined the electromagnetic interference (EMI) shielding efficiency of butyl rubber single-walled CNT (BR-SWCNT) composites made by solution mixing technique for flexible electrostatic discharge shielding applications in the X and Ku band (8.2×10^{18} GHz) [24]. Kwon et al. created innovative conductive nitrile butadiene rubber composites by employing microscale Ag flakes and MWCNTs adorned with nanoscale silver particles (nAg-MWNTs) and discovered that a minor addition of nAg MWCNTs dramatically boosted conductivity and shielding efficacy [25–28].

Natural rubber (NR) composites supplemented with electrically conducting nanofillers have been widely studied for their superior electrical, tensile, and stiffness qualities [29,30]. As a result, NR composites supplemented with conducting nanofillers can be employed as electromagnetic interference high-performance shielding materials. Nevertheless, dispersion and distribution of conducting/conductive nanofillers strongly affects the electromagnetic shielding performance. Although dielectric properties and mechanical properties of conducting nanofillers reinforced NR composites are detrimental to high electrical conductivity, they may result in excellent shielding effectiveness and mechanical performance, which is an important attribute in many commercial applications. Research on NR-based EMI-protected nanocomposites is limited. Among available reports, by using hybrid fillers, some attempted to demonstrate the shielding effectiveness and mechanical performance of NR systems containing conducting nanofillers. For instance, Hema et al. also realized that hybridization of polyaniline and metal oxide can adjust the EMI performance [31]. In a recent paper, by applying several processing techniques, Zhan et al. prepared NR/CNT nanocomposites with high electrical conductivity and acceptable low EMI level [32]. Thus,

they dispersed CNT into NR latex, pre-crosslinked NR with CNT, post-crosslinked the foamed and prepared a closed-cell microstructure.

The rapid development of polymeric materials in recent years has been fueled by the growing significance of biobased polymers and polymer nanocomposites [33–37]. In this study, we have attempted to use unique materials that can attenuate maximum EM radiation. To achieve this, NR/CIIR nanocomposites are made by incorporating nanofillers. To the best of our knowledge, until now no study has reported the nanoparticles filled NR/CIIR composite to attenuate EM radiation. Natural rubber and chlorobutyl rubber along with different fillers, such as CNT, CNF, Nano CLAY, and CB, are mixed to produce rubber nanocomposite for EMI shielding applications under different frequency ranges. The blend of CIIR/NR of 70/30 *w*/*w* ratio was also mixed with CNT, CNF, CB, and CLAY. The influence of different fillers, filler concentrations, and polymer blends was also analyzed. In addition, the study also aims to explore the influence of the NR/CIIR composite dielectric properties of nanocomposites. In a broad frequency range including both X and Ku-band, the EM shielding parameters were examined using a vector network analyzer coupled to a coaxial setup with a wide range of frequencies. Reflection and absorption to the total SE were rigorously evaluated to determine the mechanism of shielding. The electromagnetic shielding mechanisms at work in each composite are explored with appropriate electromagnetic absorption qualities. We evaluate natural rubber hybrid nanocomposites incorporating hybrid fillers for morphology, electrical conductivity, and EMI shielding. As a result, a significant increase in shielding efficacy was achieved with no weight penalty and without losing the composites' mechanical strength and stiffness.

2. Materials and Methods

2.1. Raw Materials Used

Natural rubber (NR, ISNR 5) was supplied by the Rubber Board, Kottayam, India, and has a number average molecular weight of 3×10^5 g/mol, a weighted average molecular weight (Mw) of 7.8×10^5 g/mol and a Mooney viscosity 85 mL (1 + 4) at 100 °C. Chlorobutyl rubber, Mooney viscosity ML (1 + 8) at 125 °C, with chlorine content 1.26 ± 0.08 wt% used in this study was from EXXON MOBIL (Grade: ISNR-5), which was supplied by Apollo tires. The organically modified montmorillonite used in this present study was Cloisite 10A (montmorillonite with organic modification dimethyl, benzyl, and one alkyl tail, i.e., hydrogenated. Tallow (HT) (65 m%. C18, 30 m%. C16, 5 m%. C14) modification provided by Southern Clay Products. The cation exchange capacity (CEC) was equal to 125 meq/100 g and the average dry particle size was in the range of 2 μm of −13 μm. The carbon black used was of grade ISAF and was provided by MRF. The solvents used were xylene, toluene, and hexane. MWCNTs were obtained from Nanocyl, Belgium.

2.2. Fabrication Processing

The preparation and processing techniques are mainly concentrated on different filler loading, and nature of filler, filler-type blend NR, CIIR and the blend of NR and CIIR along with different fillers, such as CNT, CNF, CB, and CLAY, are mixed in different ratios listed in the below tables (Tables 1 and 2), under a speed of 60 rpm for the preparation of various samples at a temp of 160 °C for 10–15 min using Haake Rheocord. Molding of the sheets was conducted under the temperature of 160 °C for 6 min in compression molding by using the mold of am thickness and analyzed.

This study mainly elaborates on the influence of rubber nanocomposite with different nanofillers and its different compositions, for the electromagnetic shielding of different electronic components under different frequency ranges. NR/CIIR-CB-CNT composites prepared by conventional Haakhe mixing were well dispersed, robust, and functional. The dielectric permittivity and conductivity of the NR/CIIR-CB-CNT composites were proportional to fraction and frequency, as expected. Due to fine dispersion and the creation of three-dimensional continuous networks in the matrix, the composites have a stable high

dielectric constant and AC conductivity over a wide frequency range. Figure 1 shows the schematic representation for the synthesis of NR/CIIR-based polymer nanocomposites.

Table 1. Composition of rubber nanocomposite with different nanofillers to fillers.

SL.NO	NR	CIIR	CLAY	CNT	CNF	CB (phr)	Ni (phr)
1	100	-	-	-	-	-	-
2	-	100	-	-	-	-	-
3	30	70	-	-	-	-	-
4	100	-	5	-	-	-	-
5	-	100	5	-	-	-	-
6	30	70	5	-	-	-	-
7	100	-	-	5	-	-	-
8	-	100	-	5	-	-	-
9	30	70	-	5	-	-	-
10	100	-	-	-	5	-	-
11	-	100	-	-	5	-	-
12	30	70	-	-	5	-	-
13	100	-	-	-	-	5	-
14	-	100	-	-	-	5	-
15	30	70	-	-	-	5	-
16	100	-	-	-	-	-	5
17	-	100	-	-	-	-	5
18	30	70	-	-	-	-	5
19	100	-	-	5	-	-	-
20	-	100	-	7.5	-	-	-
21	30	70	-	10	-	-	-

Table 2. Composition of rubber nanocomposite with different filler loading.

SL.NO	NR (phr)	CIIR (phr)	CNT (phr)
1	100	-	5
2	100	-	7.5
3	100	-	10
4	-	100	5
5	-	100	7.5
6	-	100	10
7	30	70	5
8	30	70	7.5
9	30	70	10

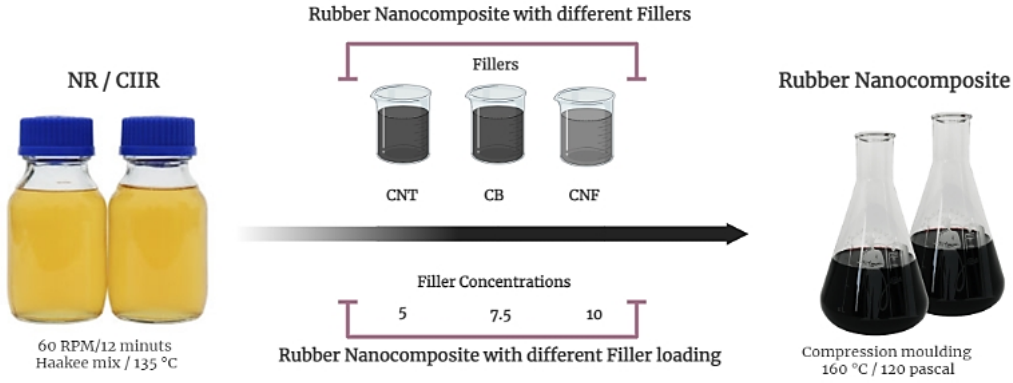

Figure 1. Scheme for the synthesis of NR/CIIR-based polymer nanocomposites.

2.3. Dielectric Permittivity and Dielectric Loss Measurements

Dielectric spectroscopy, also known as electrochemical impedance spectroscopy (EIS), evaluates the dielectric characteristics as a function of frequency and can be used to measure dielectric permittivity and dielectric loss. It is based on the interaction of an external field with the sample's electric dipole moment, which is frequently represented in terms of permittivity. Dielectric spectroscopy is an experimental method of characterizing electrochemical systems. This technique measures the impedance of a system over a range of frequencies, allowing the frequency response of the system to be observed and calculated, as well as the energy storage and dissipation properties. The samples were cut into circular discs of 12 mm diameter for dielectric property measurements in the frequency range of 100 KHz–8 MHz and put between two copper plates of the same diameter to construct a capacitor. The capacitance and loss tangent can be determined using an impedance analyzer. The data were collected on a personal computer by connecting it to LabVIEW software through a GPIB cable. The formula for calculating dielectric permittivity can be found here [38].

$$\varepsilon' = Cd/\varepsilon 0A \quad (1)$$

The dielectric loss can also be calculated by using the formula:

$$\varepsilon'' = \varepsilon' \tan \partial \quad (2)$$

where ε' is the dielectric permittivity of the sample (real part), C is the capacitance of the sample when it is inserted inside the metal plates and d is the thickness of the sample, ε_0 is the permittivity of free space, and ∂ is the loss tangent [39]. The conductivity (Ca_c) was calculated by

$$Ca_c = \dot{\omega}_0 \, \varepsilon' \tan \partial \quad (3)$$

where $\dot{\omega}$ is equal to 2ΠF (f—frequency) and ε_0 is the vacuum permittivity and ε' is the dielectric permittivity [40].

2.4. Different Composite Materials for EMI Shielding

Mostly carbon fiber, stainless steel fiber, or nickel-coated carbon fiber in a thermoplastic matrix is used to offer the necessary shielding for different equipment. Typical materials used for electromagnetic shielding consist of sheet and metal forms. Any holes in the shield or mesh must be significantly smaller than the wavelength of the radiation that is being kept out, or the enclosure will not effectively approximate an unbroken conducting surface. Polymer matrix composite containing conducting fillers is more concerned with EMI shielding property. The polymer matrix is electrically insulating in nature and does not contribute to shielding, but the incorporation of conductive fillers can make it used for shielding applications. In applications where electromagnetic compatibility is required, thermoplastic compounds for EMI/RFI shielding offer reliability and value. These unique compounds provide incredible versatility to designers and processors, as well as significant

advantages over metal, unfilled resins, and coatings. Rubber nanocomposite can also be used to guard against EMI. By integrating different fillers, various types of rubbers can be employed for EMI shielding applications such as NR and CIIR. Figure 2 represents the schematic representation of the interaction between ionic NR/CIIR and CNT-CB.

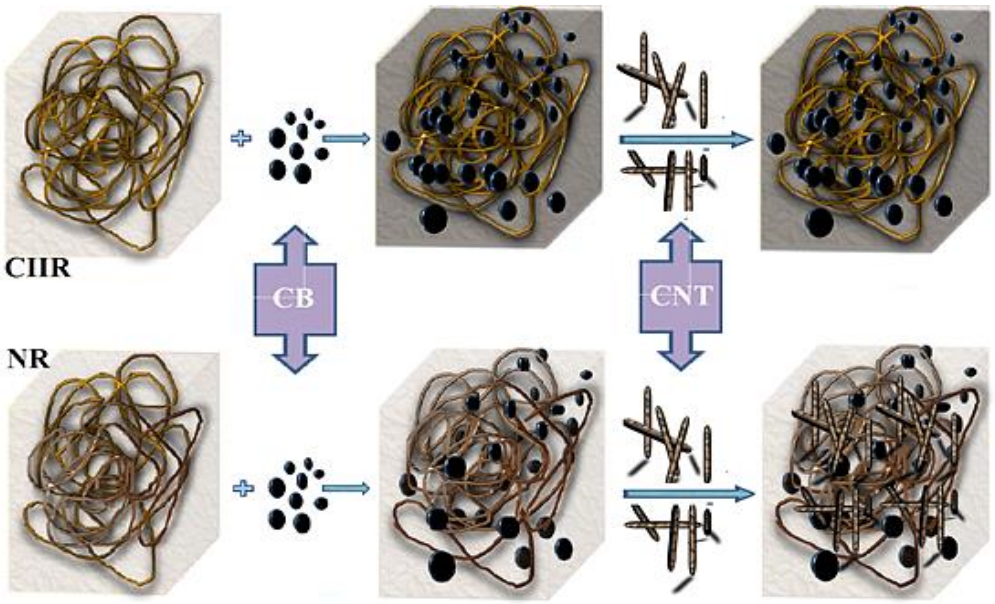

Figure 2. Schematic representation of the interaction between ionic NR/CIIR and CNT-CB.

2.5. Characterization

2.5.1. Scanning Electron Microscopy (SEM)

An environmental scanning electron microscope (PHILIPS XL30 ESEM FEG, FEI Philips, Eindhoven, The Netherlands) with a 20 kV accelerating voltage was used to examine the cryogenically fractured surface and smooth cut surface of the blend samples.

2.5.2. FTIR Spectroscopy

FTIR characterization was conducted for the analysis of the bond present in the given solid sample by using Burker (600–4000 cm^{-1}).

2.5.3. Atomic Force Microscope (AFM)

The AFM images of the cut surface of the samples were taken in tapping mode by the Dimension 3100 Nanoscope, silicon–SPM sensors with a spring constant of ca.40 N/m, and the resonance frequency of 280 KHz used with a tip radius of 10 nm was conducted by AFM APE research.

2.5.4. Dielectric Measurements

Dielectric measurements were taken for the investigations of the breakdown electric field by Precision Impedance Analyzer (Wayne Kerr Electronic—6500 B series), with the lower electrode connected to the earth and the upper electrode receiving a rising ac voltage (60 KHz) at a rate of 1 KV/s. In all circumstances, the sample thickness is 2 mm. At room temperature, permittivity and loss tangent were measured at discrete frequencies ranging from 1 Hz to 1 MHZ.

2.5.5. EMI Shielding

EMI shielding was conducted by Vector Network Analyzer in the S-band (2.7–3.9 GHz) frequency for the thickness of 2 mm with a 10 × 7 mm sample size. Resistance was measured by Resistivity Measurement Setup (70–530 K). The mechanism of shielding was systematically assessed by evaluating the reflection and the absorption contribution to

the total SE over a wide range of frequencies. The electromagnetic shielding mechanisms operating in each composite are investigated with the aim of preparing materials with suitable electromagnetic absorption properties.

3. Results and Discussion

3.1. Morphology

3.1.1. SEM

The surface morphology of natural rubber hybrid nanocomposites incorporating hybrid fillers has been carried out by using SEM. The analysis was performed in nanocomposites containing NR-CIIR-CNF, NR-CIIR-CB, NR-CIIR-CNT, and NR-CIIR-CLAY in order to evaluate the state of dispersion of the fillers and dispersed-phase NR in the CIIR matrix. From the spectra, it is clear that the fillers have got even dispersion in the polymer matrix and the two phases of NR and CIIR are visible very clearly. Figure 3 displays the photomicrographs seen in the SEM of NR-CIIR blend rubber nanocomposite.

The dispersion of the fillers was one of most important factors that contributed to the strengthening of the nanocomposites. If a lot of agglomeration and a low degree of dispersion occurred, the reinforcing effect could not be attained completely. Even though this observation was attributed to the better dispersion of fillers in the NR matrix, the white region shows that aggregated structures were not well dispersed and were wetted efficiently by the rubber matrix and agglomerated. The grey phase shows the clear dispersion of fillers in the NR/CIIR matrix.

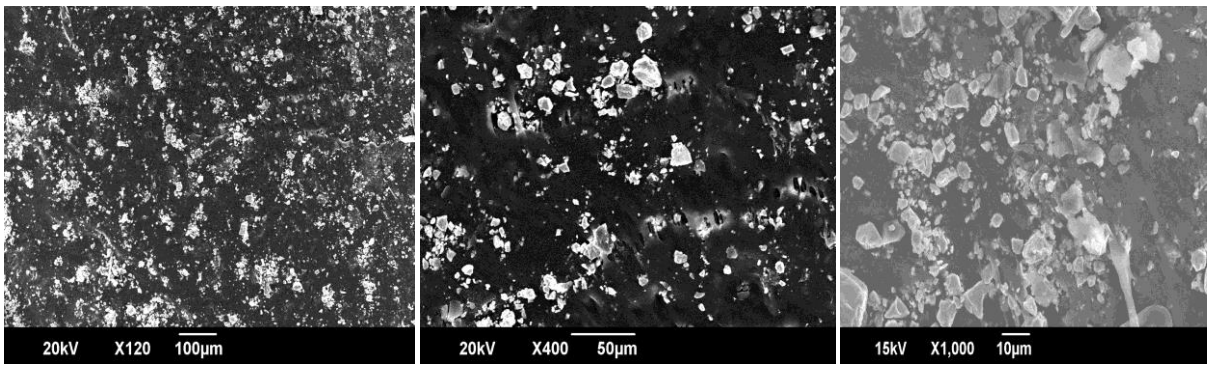

1. **NR-CIIR-CNF(5)**

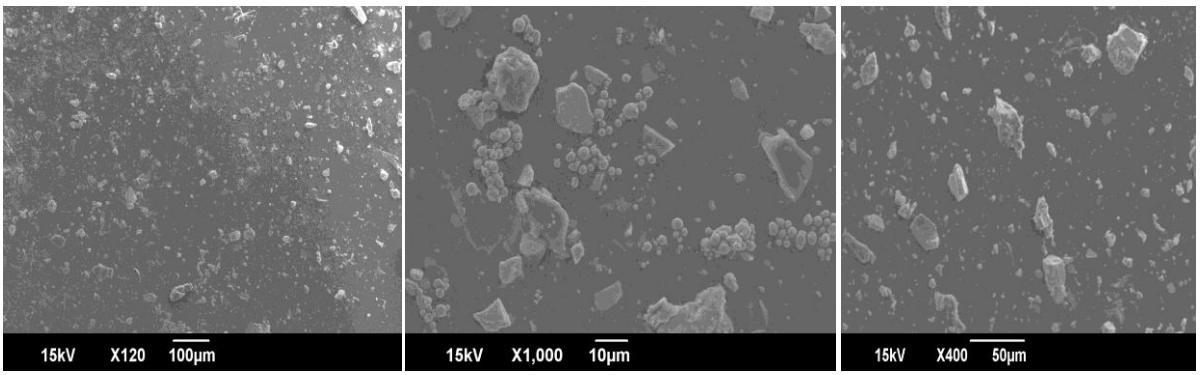

2.**NR-CIIR-CB(5)**

Figure 3. *Cont.*

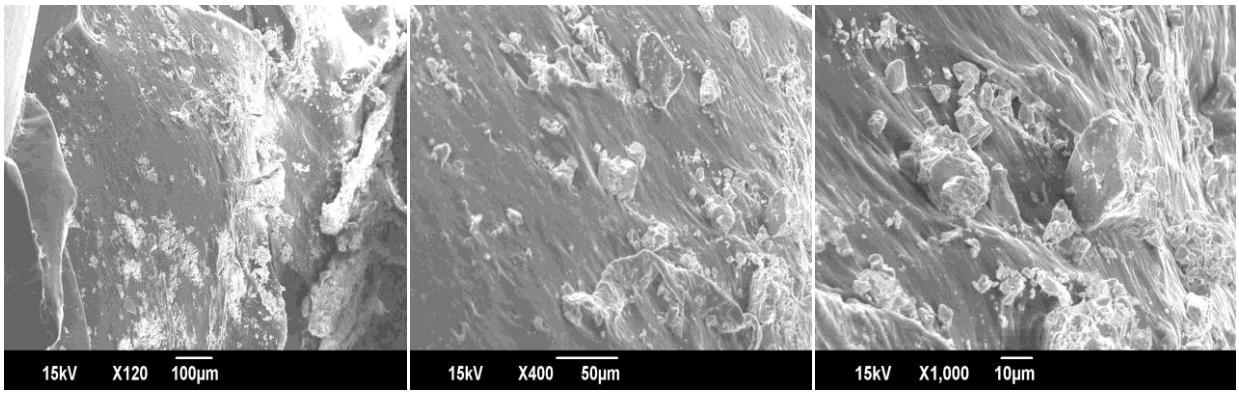

3.**NR-CIIR-CNT(5)**

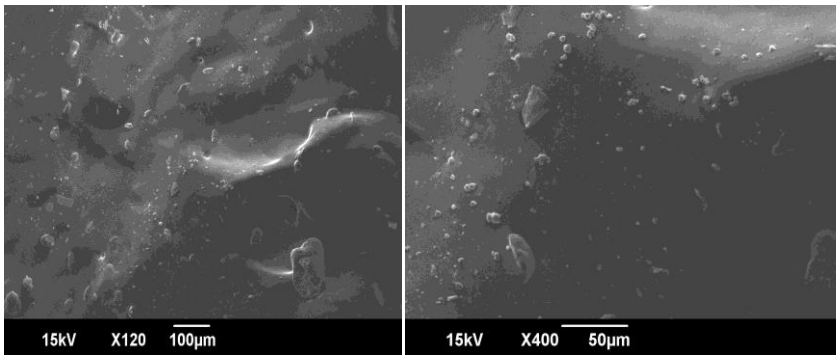

4.**NR-CIIR-CLAY(5)**

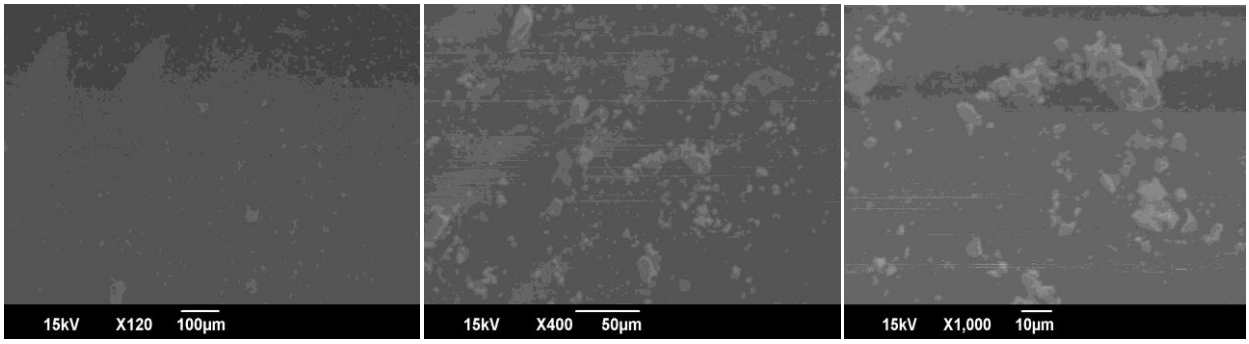

5.**NR-CIIR**

Figure 3. The SEM image of NR-CIIR blend rubber composite of different fillers.

With the direct observation of the surface morphology and tubular structure of both CNT and CNT incorporated NR/CIIR, it can be observed that the carbon nanotubes with diameters of about 100 nm are distributed very well. After the modification of NR/CIIR by CNT, there was a uniform covering of NR/CIIR on the surface of CNT. In addition to this, the morphology of CNTs in the composite is observed to have remained undamaged. No destruction of the structural integrity of CNTs is observed, which indicates that the CNTs are strong enough to withstand the functionalization process. The CNT-CB composition used here could disperse well for NR/CIIR and the results obtained are inconsistent. The interaction between ionic NR/CIIR and CNT-CB is depicted in the schematic diagram in Figure 3. The shearer force produced during the grinding of CNT and CB detaches bundles of nano compounds to individual ones.

3.1.2. Fourier-Transform Infrared Spectroscopy (FTIR)

FTIR spectroscopy has been carried out for rubber nanocomposite with different fillers in various concentrations. The blank CIIR has C=C and C=O, bonds, and by the addition of it into the CIIR polymer matrix, C-H, Cand =C, and O-H bonds can be observed and there is also a broadening of the peak at the O-H bond. For the higher filler loading of CIIR-CNT (7.5), C=O, C=C, and O-H can be observed, which is similar to neat CIIR. However, for CIIR-CNT (10), the similar bonds to CIIR-CNF (5) are observed, and there is also a broadening of the peak at the O-H bond. The CIIR-CNT (5) obtained a greater number of bonds such as C-N, C-H, C=C, C-H and O-H, which shows some interactions in the polymer matrix. Figure 4 shows the FTIR image of CIIR rubber nanocomposite with different fillers, such as CNT and CNF, in various concentrations.

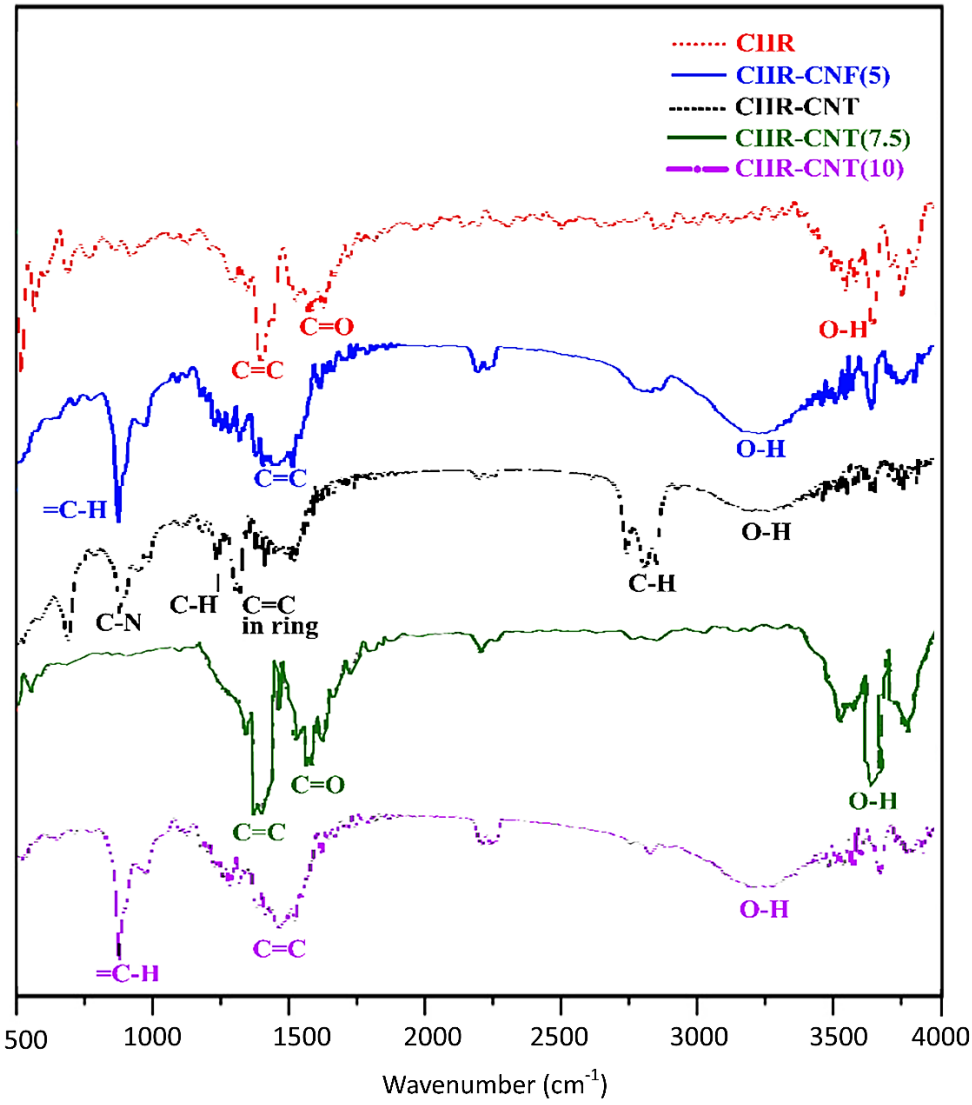

Figure 4. FTIR spectra of CIIR with different fillers CNT/CNF in different concentrations.

Blank NR and CIIR have similar bonds, such as C=O, C=C, and O-H bonds. NR-CB (5) and NR-CNT have a greater number of bonds such as C-N, C-H, C=C and, O-H and, from this, we can conclude there are some interactions, which will enhance the property of the polymer matrix. NR-CNT (5) has got bonds such as C=O, C=C and O-H, from which we can conclude for CNT that CIIR polymer has good interactions with the NR polymer matrix. Figure 5 FTIR image of NR with different fillers CNT/CNF/CB/CLAY.

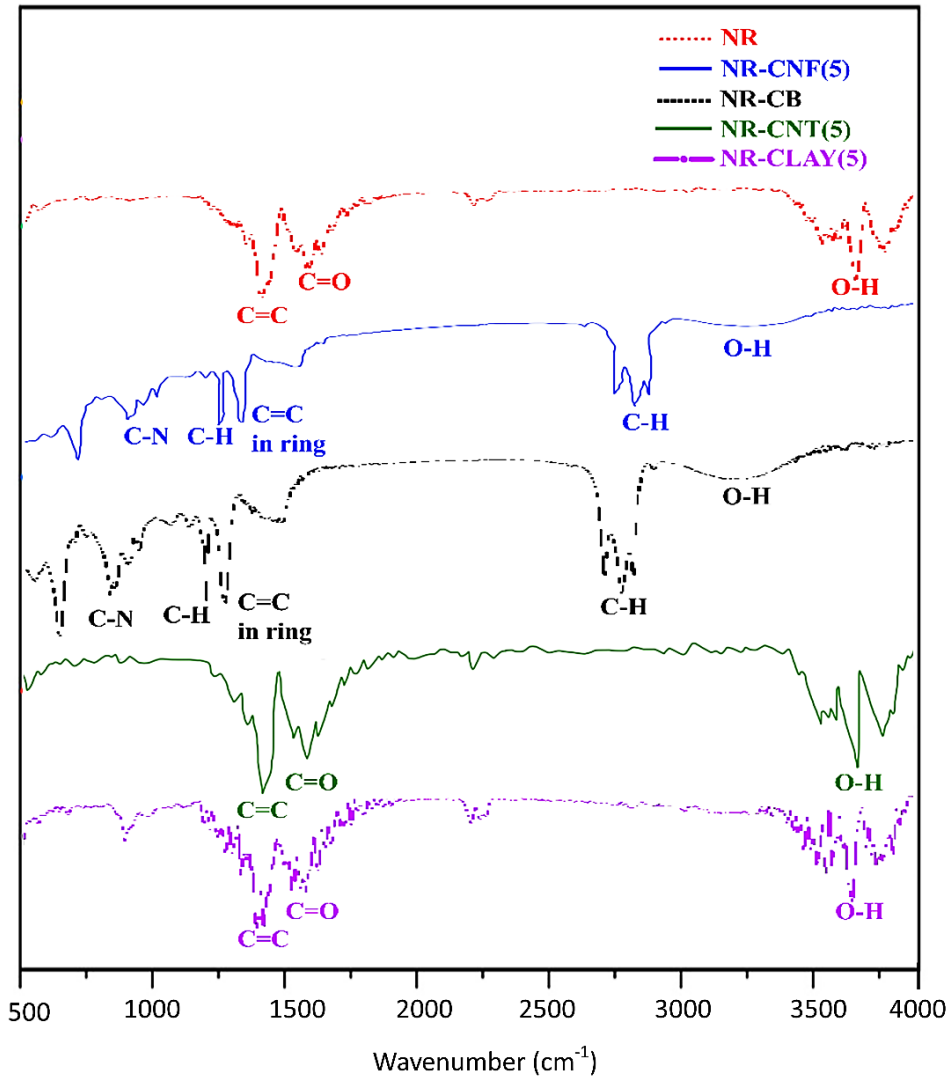

Figure 5. FTIR image of NR with different fillers CNT/CNF/CB/CLAY.

The blend nanocomposite of clay and CB shows similar bonds, such as C=O, C=C, O-and H. CIIR-NR-CNF (5) has got different bonds, such as C−H, C=C, and O-H, with a broadening of the peak at the O-H bond. Similar bonds, such as C=C, C=O, and O-H, can be observed for the different concentrations of CNT in the blend polymer co−mposite. Since the blend composite NR-CIIR-CNT (5) has got a greater number of bonds, there are good interactions in between to improve the property of the polymer blend. From the FTIR spectroscopy results, it is evident that the combinations NR-CB (5), CIIR-CNT (5), NR-CIIR-CNT (5), and NR-CNF (5) have some interaction since it shows a greater number of bonds such as C-N, C-H, C=C, C-O, and O-H. Figure 6 shows the FTIR image of CIIR-NR blend nanocomposite with different fillers.

3.1.3. AFM

AFM image of the surface of a composite after coagulation of the latex beads at 60 °C. The derivative of topography signal is shown to highlight the morphology of the film after water evaporation. The AFM image shows that in CIIR-CB (20)-CNT (5) the fillers have got even dispersion in the polymer matrix for the best result of EMI shielding of 59 dB. It was not possible to resolve individual nanotubes at the composite surface. No clusters of CNT were observed, either, showing that macroscopic dispersion was good. Figure 7 shows the AFM image of CIIR-CB (20)-CNT (5), the best result for EMI shielding of 59 db.

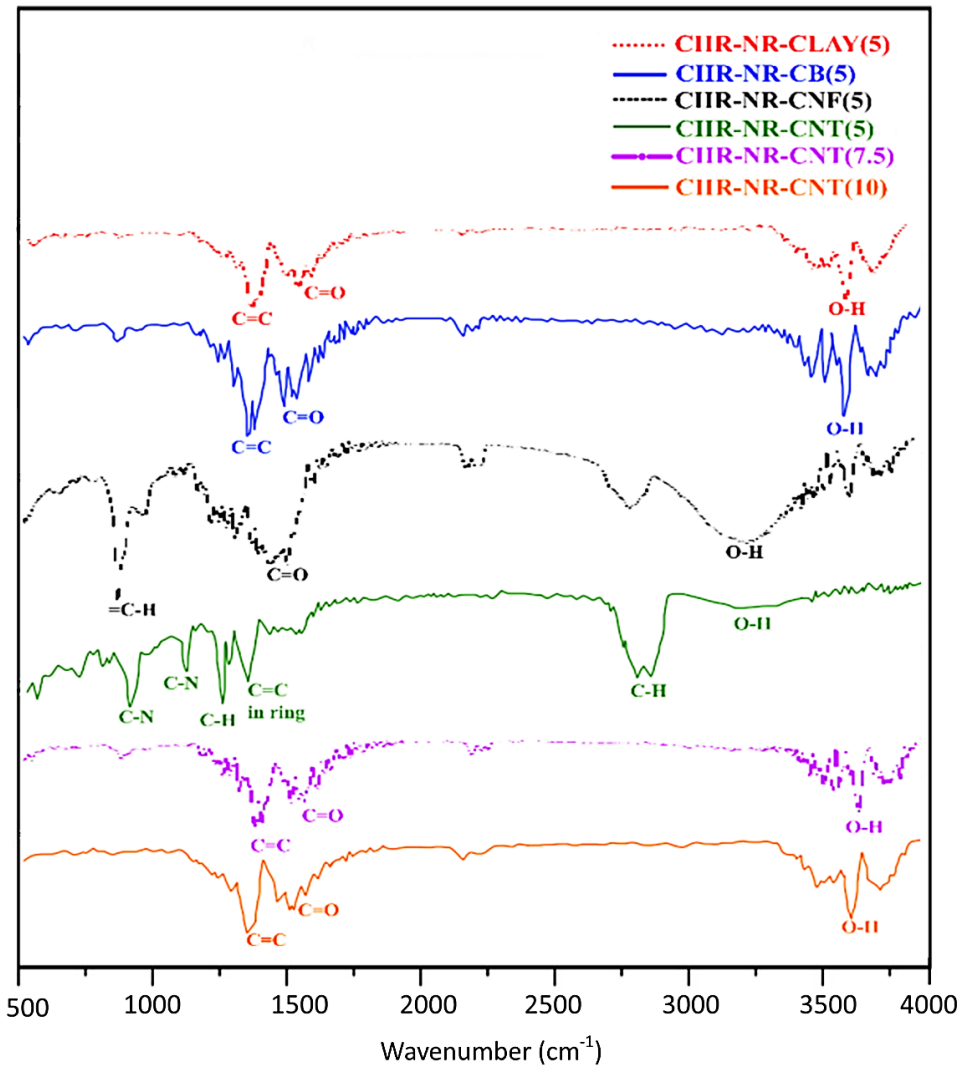

Figure 6. FTIR image of CIIR-NR blend nanocomposite with different fillers CNT/CNF/CB/CLAY with different concentrations.

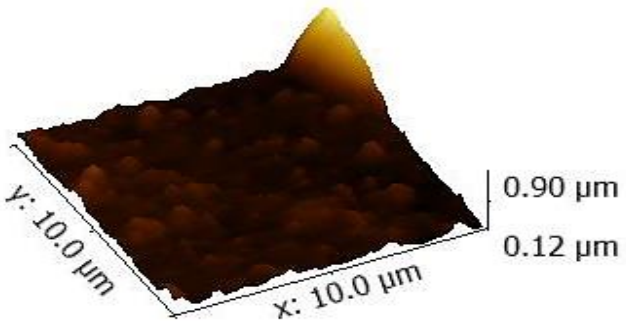

Figure 7. AFM image of CIIR-CB (20)-CNT (5), the best result for EMI shielding of 59 db.

3.2. Resistivity Meter

From the resistivity–composition graph of hybrid filler composition and blend rubber nanocomposite in NR/CIIR matrix, it can be observed that compared to neat NR, the conductivity of the NR-CIIR blend has got higher value. When compared with blank NR and NR-CIIR blend, blank CIIR has got higher value for conductivity. By the addition of fillers such as CNT, CB, CLAY and CNF, we can observe that the conductivity of both CIIR and CIIR-NR has increased to a good extent, because of the good dispersion of fillers in the

polymer matrix. The lower viscosity of CIIR also should have a role in the good dispersion of filler in the polymer matrix. The high-temperature mixing also enhances the conductivity of the polymer matrix by about 40%, which may be due to the better dispersion of the nanofiller at high-temperature mixing. From the above graph, we can conclude, that the influence of filler concentration also affects the conductivity of the polymer matrix. Figure 8 shows the relation of resistivity by different compositions of polymer nanocomposite.

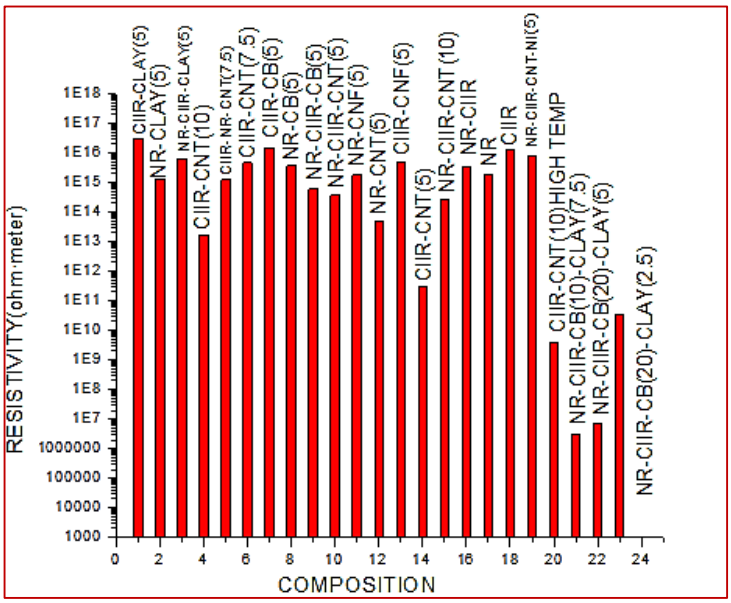

Figure 8. Resistivity–composition graph of hybrid filler composition and blend rubber nanocomposite in NR/CIIR matrix.

The study shows that, CIIR-NR-CB (20)-CLAY (7.5) increase the conductivity of the polymer matrix. High-temperature mixing and the mixing methodology (solution mixing) also enhance the conductivity of the polymer matrix. Figure 9 shows that the hybrid filler composition CIIR-CB (20)-CNT (5) and the blend rubber nanocomposite.

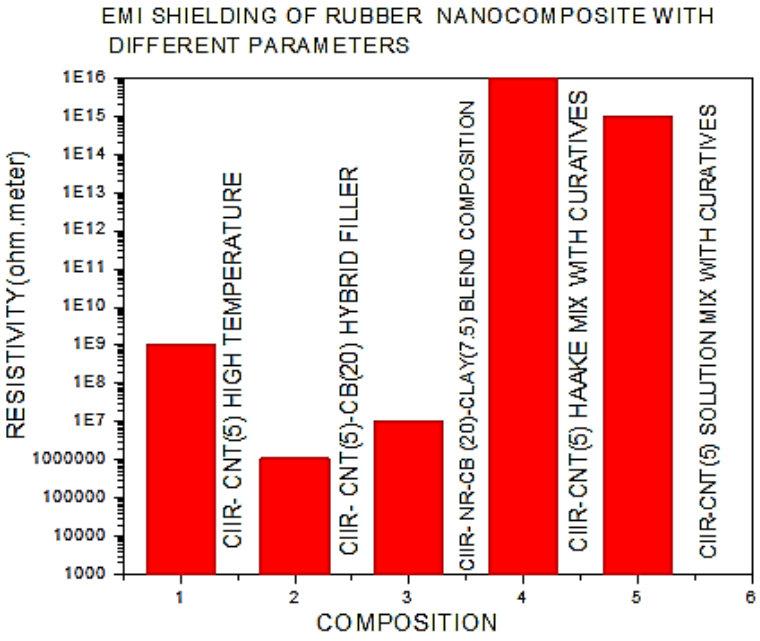

Figure 9. Resistivity–composition graph of hybrid filler composition and blend rubber nanocomposite in NR/CIIR matrix.

3.3. Conductivity

From the study, it is observed that CIIR-NR-CLAY (5) and CIIR-NR-CNF obtained high AC conductivity and CIIR-NR-CB obtained low AC conductivity. CIIR-CNT (5) and CIIR-CNF obtained high AC conductivity because of good dispersion in CIIR and CIIR-NR-CB obtained low AC conductivity. NR-CNT (5) obtained high AC conductivity because of good dispersion in NR and CIIR-NR-CB obtained low AC conductivity. Figure 10 shows the AC conductivity of CIIR/NR blend, CIIR, and NR rubber nanocomposites with different fillers.

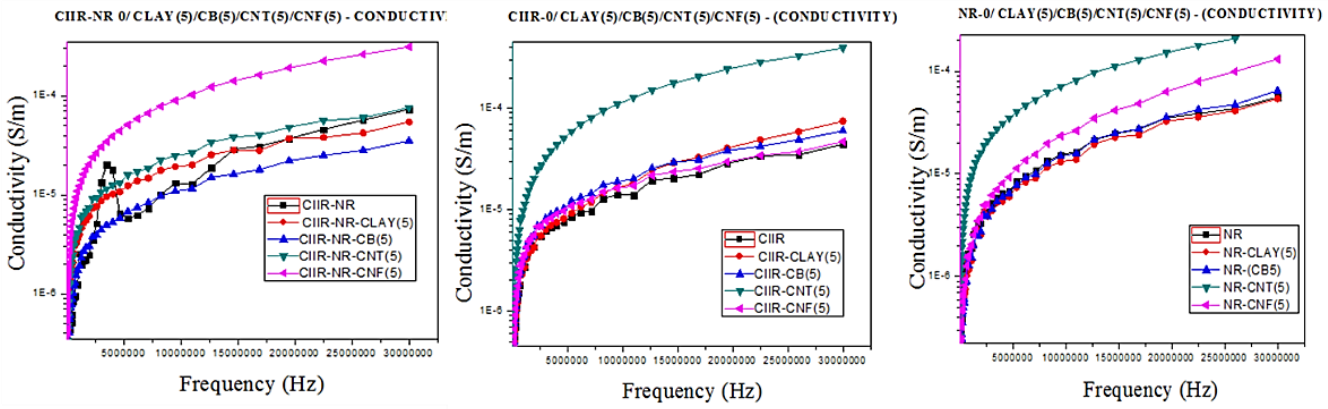

Figure 10. AC conductivity of CIIR/NR blend, CIIR, and NR rubber nanocomposites with different fillers.

The study reveals that AC conductivity on the blend system will work more for CIIR and NR with CNT. For the blend system, the filler concentration of 10 and 5 phr showed good conductivity.

CIIR-CNT (10) > CIIR-CNT (5) > CIIR-CNT (7.5) > CIIR–AC conductivity
CIIR-NR-CNT (10) > CIIR-NR-CNT (5) > CIIR-NR-CNT (7.5) > NR-CIIR–AC conductivity

Figure 11 shows the frequency dependencies of AC conductivity of CIIR and CIIR-NR-CNT rubber nanocomposite with different filler concentrations.

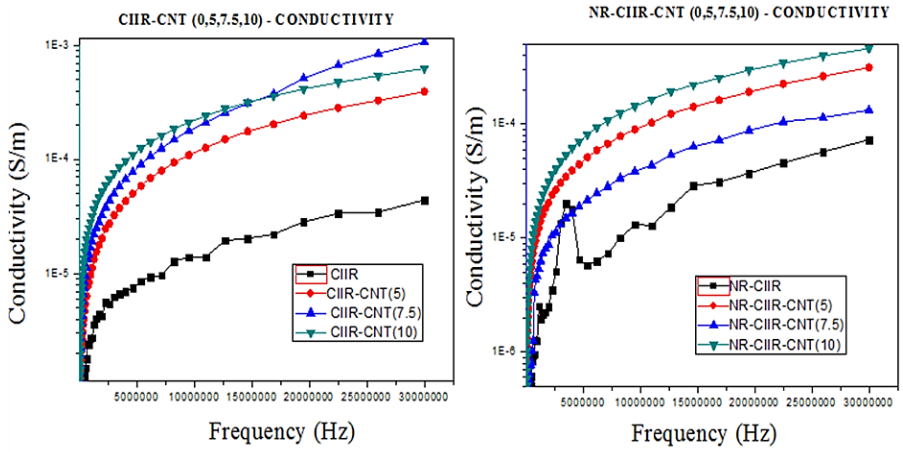

Figure 11. Frequency dependencies of AC conductivity of CIIR and CIIR-NR-CNT rubber nanocomposite with different filler concentrations.

3.4. Dielectric Properties

3.4.1. Dielectric Permittivity

The permittivity of a medium describes how much electric field (more correctly, flux) is 'generated' per unit charge in that medium. In CIIR-NR blend, the fillers CNT and CNF have high permittivity and the blend of NR-CIIR and CIIR-NR-CB has very low permittivity.

For CNT and CNF, more electricity is generated per unit charge, in the medium. So, NR-CIIR-CNF and NR-CIIR-CNT have high EMI shielding and it is very conducive in nature when compared to the other fillers incorporated in the NR-CIIR blend. Figure 12 shows the frequency dependencies of dielectric permittivity of CIIR/NR blend, CIIR and NR rubber nanocomposites with different fillers.

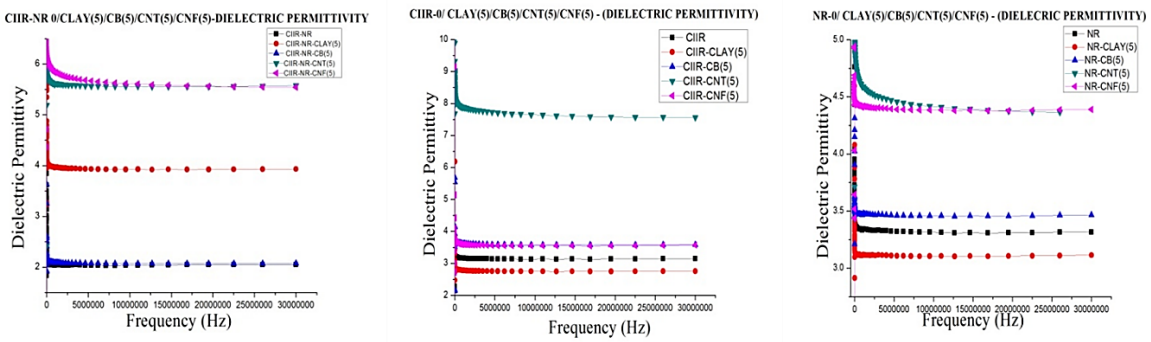

Figure 12. Frequency dependencies of dielectric permittivity of CIIR/NR blend, CIIR and NR rubber nanocomposites with different fillers.

In CIIR, the fillers CNT and CNF has high permittivity and blank CIIR and CIIR-CLAY have very low permittivity. For CNT and CNF, more electricity is generated per unit charge, in the medium. So, CIIR-CNF and CIIR-CNT have high EMI shielding and it is very conducive in nature when compared to the other fillers incorporated in CIIR. It shows a similar trend as in blend with an exception in CLAY.

In NR, the fillers CNT and CNF have high permittivity and blank NR and NR-CLAY have very low permittivity. For CNT and CNF, a greater number of electricity is generated per unit charge, in the medium. So, NR-CNF and NR-CNT have high EMI shielding and it is very conducive in nature when compared to the other fillers incorporated in CIIR. It shows a similar trend as in blend; the exception is only for CLAY. Figure 13 shows the frequency dependencies of dielectric permittivity of CIIR and NR/CIIR blend rubber nanocomposites with different filler concentrations.

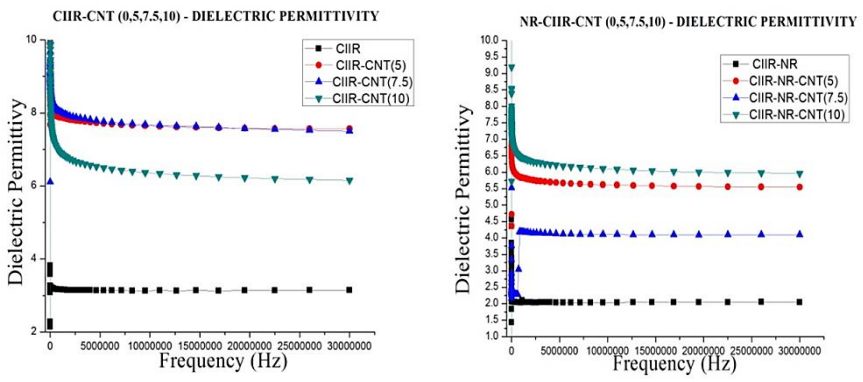

Figure 13. Frequency dependencies of dielectric permittivity of CIIR and NR/CIIR blend rubber nanocomposites with different filler concentrations.

In CIIR, the filler concentration of 7.5 and 5 has high permittivity because of good dispersion, and when it comes to the filler concentration of 10, there is less permittivity because of agglomeration. So, the filler concentration of 5 and 7.5 has high EMI shielding and it is very conducive in nature. In the CIIR-NR blend, the filler concentration of 10 and 5 has high permittivity because of good dispersion. So, the filler concentration of 5 and 10 has high EMI shielding and it is very conducive in nature.

3.4.2. Dielectric Loss

Dielectric loss quantifies a dielectric material's inherent dissipation of electromagnetic energy. The blend combination of NR-CIIR-CNT and CIIR-NR-CB has less dielectric loss, so it has less dissipation of electromagnetic energy and it has good EMI shielding, and also it has high dielectric permittivity. The combination of CIIR-CLAY, and CIIR-CB has less dielectric loss, so it has less dissipation of electromagnetic energy and it has good EMI shielding, and also it has high dielectric permittivity. CIIR-CNT has a high dielectric loss. The combination of NR-CNF, and NR-CB has less dielectric loss, so it has less dissipation of electromagnetic energy and it has good EMI shielding, and also it has high dielectric permittivity. NR-CNT and blank NR has a high dielectric loss. Figure 14 shows the frequency dependencies of dielectric permittivity of CIIR/NR blend, CIIR and NR rubber nanocomposites with different fillers.

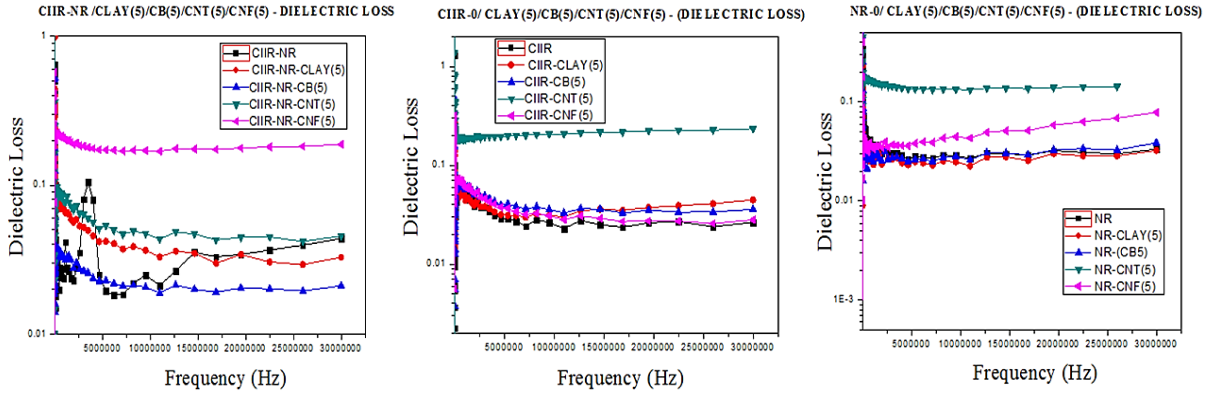

Figure 14. Frequency dependencies of dielectric permittivity of CIIR/NR blend, CIIR and NR rubber nanocomposites with different fillers.

The filler concentration of 5 and 7.5 in CIIR has less dielectric loss, so it has less dissipation of electromagnetic energy, good EMI shielding, and high dielectric permittivity. The filler concentration of 10 phr in CIIR has high dielectric loss because of agglomeration. The filler concentration of 7.5 phr in NR-CIIR has less dielectric loss, so it has less dissipation of electromagnetic energy, good EMI shielding, and high dielectric permittivity. The filler concentration of 10 and 5 phr in NR-CIIR has a high dielectric loss. The dielectric loss of rubber nanocomposite with the influence of hybrid filler and blend composition also attributes similar kinds of dielectric loss. For the NR/CIIR blend, CNT and CB obtained a high dielectric loss. In CIIR and NR, the CNF and CNT show a high dielectric loss. In CIIR and the blend of CIIR/NR, the filler concentration of 10 phr shows a high dielectric loss. Figure 15 shows the dielectric loss tangent frequency dependencies of CIIR and CIIR/NR rubber nanocomposites with different filler concentrations.

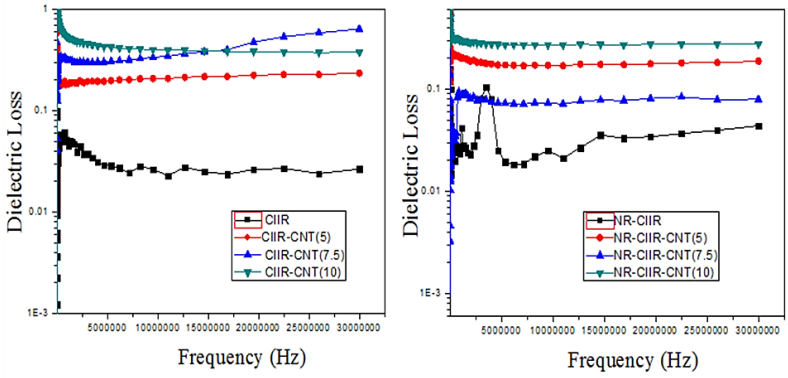

Figure 15. Dielectric loss tangent frequency dependencies of CIIR and CIIR/NR rubber nanocomposites with different filler concentrations.

3.5. EMI Shielding

Electromagnetic shielding is the practice of reducing the electromagnetic field in a space by blocking the field with barriers made of conductive or magnetic materials. The shielding can reduce the coupling of radio waves, electromagnetic fields, and electrostatic fields. In the low-temperature mixing of blends, NR-CIIR-CNT (5) got 10 dB, NR-CIIR-CNF (5) got 10 dB and NR-CIIR-CLAY (5) got 2 dB. Figure 16 shows the EMI shielding effectiveness frequency dependencies of CIIR-NR, CIIR, and NR rubber nanocomposites with different filler and Figure 17 shows the EMI shielding effectiveness frequency dependencies of CIIR and CIIR/NR blend rubber nanocomposites with different filler concentrations.

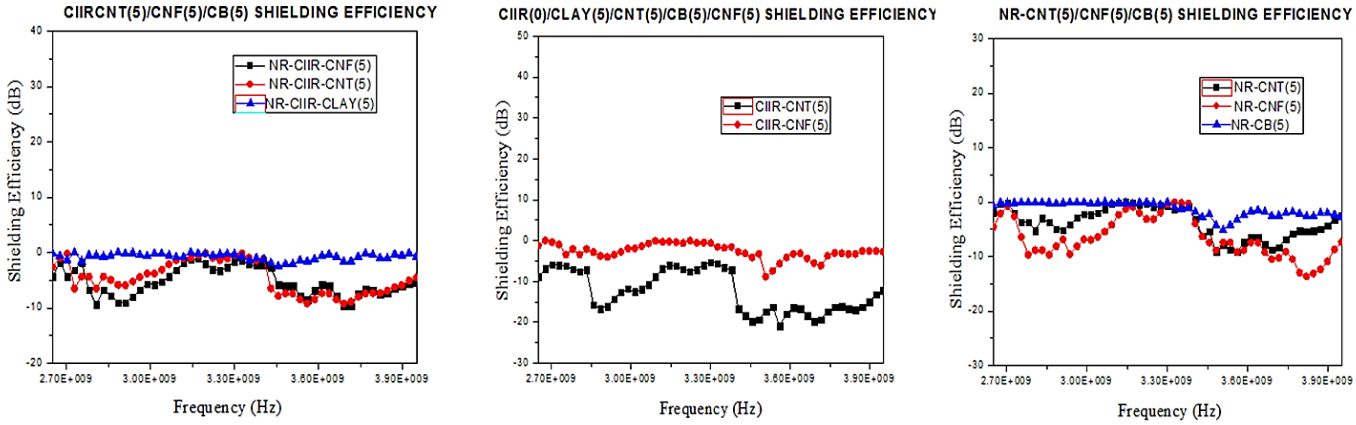

Figure 16. EMI shielding effectiveness frequency dependencies of CIIR-NR, CIIR, and NR rubber nanocomposites with different filler.

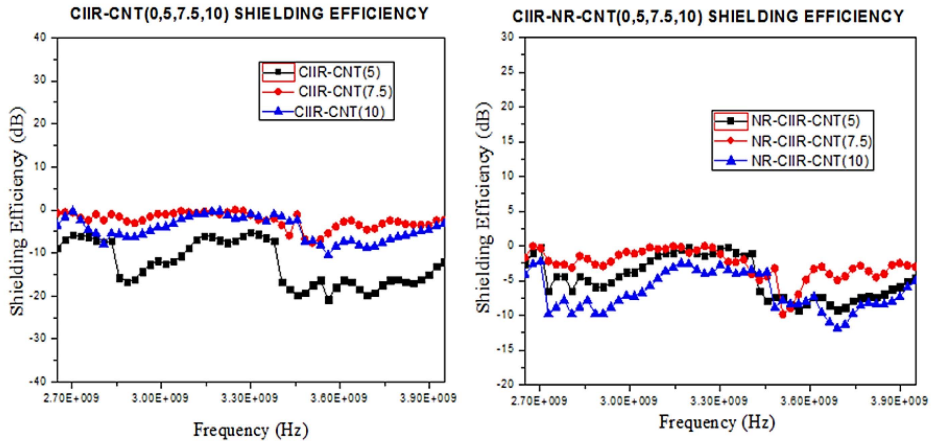

Figure 17. EMI shielding effectiveness frequency dependencies of CIIR and CIIR/NR blend rubber nanocomposites with different filler concentrations.

In the low-temperature mixing of different filler concentrations, CIIR-CNT (5), CIIR-CNT (10) and CIIR-CNT (7.5) obtained 25, 12, and 10 dB, respectively. At the low-temperature mixing of different filler concentrations, NR-CIIR-CNT (5), CIIR-CNT (10) and CIIR-CNT (7.5) obtained 10, 13, and 12 dB respectively. Figure 18 shows the EMI Shielding versus composition graph of rubber nanocomposite with different fillers.

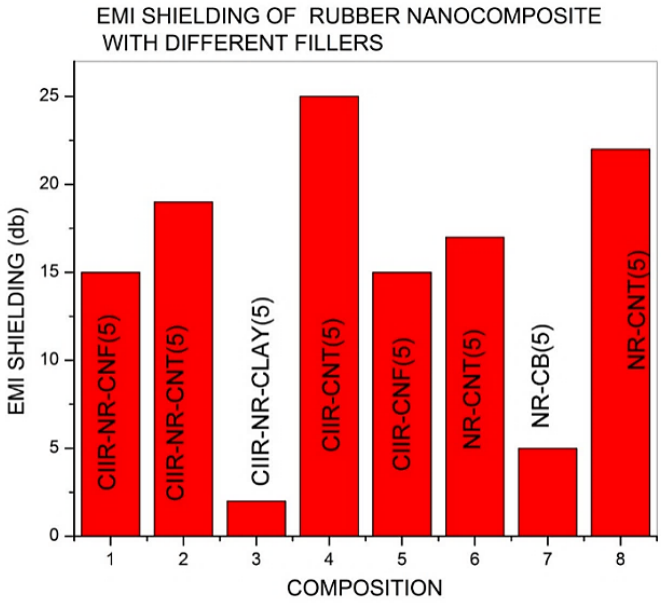

Figure 18. EMI Shielding versus composition graph of rubber nanocomposite with different fillers.

CIIR shows the best results for EMI shielding when compared to the blend system and plane NR. The fillers CNT and CNF showed the good values of EMI shielding. Temperature and time of mixing have a great role in increasing the EMI shielding of the material. An increase in the time of mixing and temperature linearly increases the EMI shielding of the material. An increase in the filler loading also positively influences the shielding but due to the great chances for the agglomeration, it may negatively influence the EMI shielding. Figure 19 shows the EMI shielding versus composition graph of rubber nanocomposite with different filler concentrations.

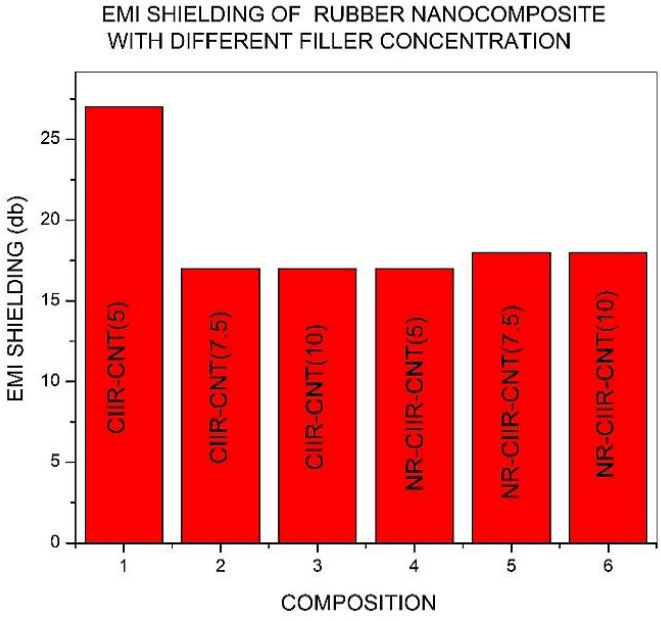

Figure 19. EMI shielding versus composition graph of rubber nanocomposite with different filler concentrations.

Both the average SET and the AC conductivity values were plotted with CNT concentration to link the EMI shielding properties with the electrical properties. Since most commercial applications of EMI shielding fall within the GHz frequency range, EMI shielding research has been conducted in this frequency range. The interconnected network of

conducting particles is the primary need for microwave attenuation in polymer nanocomposites, including conducting particles. It was discovered that as the number of CNTs grew, SET increased due to better AC conductivity. Composites with 10 phr CNT have higher conductivity and SET values. As a result, electrical conductivity is one of the most important conditions for obtaining good SET values. Another crucial condition for strong EMI shielding capabilities, particularly in CNT-filled composites, is that the filler content be substantially above the PT. Multiple conducting routes were generated above PT by CNT networks, which may aid in attenuating EM waves and increasing shielding qualities. This phenomenon will be crucial in the development of future composites for EMI shielding.

The total shielding efficacy was further resolved into the reflection loss (SER) and absorption loss (SEA) components to explore the shielding mechanism. The SE due to absorption and reflection (SEA and SER) increases with increasing filler loading, according to the experimental findings. This can be accomplished by increasing the composites' conductivity. It is worth noting that the contribution of SEA to EM wave attenuation is larger than that of SER, owing to increased conductivity and dielectric losses. CNT's high SE values in NR/CIIR are due to its high aspect ratio and the creation of network-like characteristics by CNT. More surface sites are accessible for the incoming wave to engage and communicate with the entire network as a result of this. The inference is highly associated with the morphology, structure, and phase features of the experience. The incident electromagnetic wave interacts with the conducting nanofillers, facilitating electron transport (microwave absorption) across the nanocomposites via the conductive network. There are two important aspects to consider in order to be a good absorber. One is the impedance matching condition, which permits the EM wave to propagate sufficiently into the absorber while avoiding severe reflection; this is also a prerequisite for EM wave absorption. The composites' high dielectric permittivity attenuates EM radiation. The optimum EM wave attenuation performance inside the absorber is another important consideration. An excellent absorber may quickly attenuate the incident EM wave as it passes through the absorber layer, reducing the emerging wave to a manageable size. It is commonly understood that when an EM wave strikes an absorber sample, two possible contributions to EM wave absorption exist: dielectric loss and magnetic loss. The significant dielectric loss of composites facilitated the absorption of EM radiation in this case. The composite exhibits the greatest dielectric loss at a 10 phr modified CNT absorber loading, indicating that the EM wave energy may be successfully transformed into heat or other forms absorbed by materials at this content, and the EM wave is thus dampened inside the absorber. Ionic liquid improves the EM wave absorption of CNTs in this CNT-based nanocomposite absorber. The collective interfacial dipole movements at the interfaces could improve the response to incident EM waves and hence the EM wave absorption performance. As a result, dipole polarization may have a role in the dielectric loss. As a result, the contribution of absorption to the total EMI SE (95%) is substantially greater than that of reflection, implying that absorption rather than reflection dominates the shielding mechanism in CNT integrated NR/CIIR composites. Based on the findings, it can be concluded that absorption, with a modest contribution from reflection, is the predominant shielding mechanism of NR/CIIR-CNT composites. This suggests that the composites in this situation are effective EM absorbers. As a result, composites with increased electrical conductivity have higher absorption, which is backed up by CNTs' natural EM absorbing characteristics. If the shielding material has good thermal conductivity, the heat created during the attenuation of EM waves via absorption in the shielding material is dissipated as heat. CNT composites have been reported to have superior heat conductivity than neat polymers in the literature.

The dielectric constant of polymer composites depends upon the nature of filler particles. In the present study, the increased conductivity of CLAY or/and CB filled with polymer matrix composites exhibited a higher dielectric constant, because of the higher conductivity of the fillers. However, the reinforcement of CLAY results in significant increases in the dielectric constant value, which might be due to the intercalation of polymer

chains into the clay particle, which improves the polarizability of composites and the enhancement of filler–filler interaction and increases the incontinuity of the conducting phase. The report showed that the dielectric properties, such as dielectric constant, dielectric loss and volume resistivity, were studied at room temperature and found improved results of the combination of modified clay/CB filled hybrid composites [41]. It is evident from the data that stronger interfacial polarization results from improved polymer chain intercalation into clay particles and the similar trend was seen in the dielectric loss (ε''). With the increased frequency, it is evident as relaxation peaks in dielectric loss spectrum that the overall molecular mobility of nanocomposites also increases. The presence of polar groups and the conductivity of CB contributed to the enhancement of the conducting path throughout the polymer matrix, which causes the resistance to drop when filler is added.

The present study reveals that the AC conductivity on the blend system performs well for CIIR and NR with CNT since, in the blend system, the filler concentration of 10 and 5 phr showed good conductivity. This might be due to the conducting path between fillers, and due to the delamination of clay particles the tunnelling properties of electrons are enhanced.

4. Conclusions

In recent years, designing new conducting materials with promising electromagnetic shielding applications has attracted widespread attention. Styrene-butadiene rubber (SBR) is extensively used for low-cost synthetic rubber for a large number of applications, even though their use in providing an effective barrier to electromagnetic radiation is limited by their poor electrical conductivity. For overcoming this shortcoming, the electromagnetic interference (EMI) shielding effectiveness of NR/CIIR composites was studied. Natural rubber and chlorobutyl rubber along with different fillers, such as CNT, CNF, nanoclay, and CB, are mixed to produce rubber nanocomposite for EMI shielding applications. The blend of CIIR/NR in a 70/30 ratio also mixed with CNT, CNF, CB and CLAY. The influence of different fillers, filler concentration temperature, and timing for mixing is analyzed, and from the UV spectroscopy it is evident that the CIIR has its absorbance peak under the 320 nm range. From the FTIR spectroscopy, it is evident that CIIR-CNT (5), NR-CIIR-CB (5), NR-CIIR-CNT (5) has got a greater number of bonds, so it has chances for good dispersion. From the dielectric spectroscopy, it is evident that the dielectric loss, dielectric permittivity and AC conductivity favor CIIR-CNT (5) of 29 dB and CIIR-CNF (5) of 15 dB over its blend composite. There is a good influence for the filler concentration that enhances the EMI shielding but at the same time for CIIR-CNT (10) there is the chance for the agglomeration also and this negatively influences the EMI shielding property. High temperature also influences the EMI shielding, and CIIR-CNT (5), with high temperature and by increasing the mixing time, also enhances the EMI shielding. The solution mixing also enhances better dispersion than melt mixing. The hybrid filler of CIIR-CNT (5)-CB (20) has got a good shielding value of 59 dB. The blend of NR-CIIR-CB (20)-CLAY (7.5) also influences the dispersion and EMI value. It was evident by SEM and AFM analysis that there is good dispersion for the above system. The filler has good affinity towards the CIIR phase in a blend system compared to NR, and hence the EMI shielding value is high for CIIR compared to in the blend system. From the data, it was observed that, at a particular frequency, the shielding effectiveness increases with the increasing loading of carbon fiber in the composite. The results showed that 30 to 40 phr (parts per hundred parts of rubber) loading of fillers makes the rubber composite a potential EMI shielding material for use in the electronics industry. This work opens up a new paradigm for EMI shielding applications based on natural and chlorobutyl rubber blend nanocomposite with the aid of a sustainable and simplified methodology. The morphology of the blend systems is analyzed by SEM. All of our observations call for a better understanding to grant a resourceful and effective method to fabricate a potential and excellent lightweight, flexible materials for EMI shielding.

Author Contributions: T.M.J.: conceptualization, methodology, and writing—original draft preparation; H.J.M.: data curation and validation; J.T.H.: supervision and writing—review and editing; S.T.: visualization and supervision; A.E.: formal analysis; S.M.S.: writing—review and editing. All authors have read and agreed to the published version of the manuscript.

Funding: This research received no external funding.

Conflicts of Interest: The authors declare no conflict of interest.

References

1. Singh, R.; Singh, P.K. Agarose Biopolymer Electrolytes: Ion Conduction Mechanism And Dielectric Studies. Available online: https://www.semanticscholar.org/paper/AGAROSE-BIOPOLYMER-ELECTROLYTES-%3A-ION-CONDUCTION-Singh-Singh/2607511dd22f4a20904bd6f6c5df6b7e8a1be1bc (accessed on 30 June 2022).
2. Abdollahiyan, P.; Heidari, H.; Hassanzadeh, S.; Hasanzadeh, M.; Seidi, F.; Pashazadeh-Panahi, P. Providing Multicolor Plasmonic Patterns with Graphene Quantum Dots Functionalized D-Penicillamine for Visual Recognition of V(V), Cu (II), and Fe(III): Colorimetric Fingerprints of GQDs-DPA for Discriminating Ions in Human Urine Samples. *J. Mol. Recognit.* **2021**, *34*, 2936. [CrossRef] [PubMed]
3. Tan, H.W.; Choong, Y.Y.C.; Kuo, C.N.; Low, H.Y.; Chua, C.K. 3D Printed Electronics: Processes, Materials and Future Trends. *Prog. Mater. Sci.* **2022**, *127*, 100945. [CrossRef]
4. Zadeh, M.K.; Yeganeh, M.; Shoushtari, M.T.; Ramezanalizadeh, H.; Seidi, F. Microstructure, Corrosion Behavior, and Biocompatibility of Ti-6Al-4 V Alloy Fabricated by LPBF and EBM Techniques. *Mater. Today Commun.* **2022**, *31*, 103502. [CrossRef]
5. Abdollahiyan, P.; Hasanzadeh, M.; Pashazadeh-Panahi, P.; Seidi, F. Application of Cys A@AuNPs Supported Amino Acids towards Rapid and Selective Identification of Hg(II) and Cu(II) Ions in Aqueous Solution: An Innovative Microfluidic Paper-Based (MPADs) Colorimetric Sensing Platform. *J. Mol. Liq.* **2021**, *338*, 117020. [CrossRef]
6. Mobed, A.; Hasanzadeh, M.; Seidi, F. Anti-Bacterial Activity of Gold Nanocomposites as a New Nanomaterial Weapon to Combat Photogenic Agents: Recent Advances and Challenges. *RSC Adv.* **2021**, *11*, 34688–34698. [CrossRef] [PubMed]
7. Farshchi, F.; Saadati, A.; Kholafazad-Kordasht, H.; Seidi, F.; Hasanzadeh, M. Trifluralin Recognition Using Touch-Based Fingertip: Application of Wearable Glove-Based Sensor toward Environmental Pollution and Human Health Control. *J. Mol. Recognit.* **2021**, *34*, 2927. [CrossRef] [PubMed]
8. Abdollahiyan, P.; Hasanzadeh, M.; Seidi, F.; Pashazadeh-Panahi, P. An Innovative Colorimetric Platform for the Low-Cost and Selective Identification of Cu(II), Fe(III), and Hg(II) Using GQDs-DPA Supported Amino Acids by Microfluidic Paper-Based (MPADs) Device: Multicolor Plasmonic Patterns. *J. Environ. Chem. Eng.* **2021**, *9*, 106197. [CrossRef]
9. Wang, M.; Tang, X.-H.; Cai, J.-H.; Wu, H.; Shen, J.-B.; Guo, S.-Y. Construction, Mechanism and Prospective of Conductive Polymer Composites with Multiple Interfaces for Electromagnetic Interference Shielding: A Review. *Carbon* **2021**, *177*, 377–402. [CrossRef]
10. Kordasht, H.K.; Mirzaie, A.; Seidi, F.; Hasanzadeh, M. Low Fouling and Ultra-Sensitive Electrochemical Screening of Ractopamine Using Mixed Self-Assembly of PEG and Aptamer Immobilized on the Interface of Poly (Dopamine)/GCE: A New Apta-Platform towards Point of Care (POC) Analysis. *Microchem. J.* **2021**, *171*, 106853. [CrossRef]
11. Seidi, F.; Zhao, W.; Xiao, H.; Jin, Y.; Zhao, C. Layer-by-Layer Assembly for Surface Tethering of Thin-Hydrogel Films: Design Strategies and Applications. *Chem. Rec.* **2020**, *20*, 857–881. [CrossRef] [PubMed]
12. Seidi, F.; Crespy, D. Fighting Corrosion with Stimuli-Responsive Polymer Conjugates. *Chem. Commun.* **2020**, *56*, 11931–11940. [CrossRef] [PubMed]
13. Seidi, F.; Reza Saeb, M.; Huang, Y.; Akbari, A.; Xiao, H. Thiomers of Chitosan and Cellulose: Effective Biosorbents for Detection, Removal and Recovery of Metal Ions from Aqueous Medium. *Chem. Rec.* **2021**, *21*, 1876–1896. [CrossRef]
14. Marandi, A.; Nasiri, E.; Koukabi, N.; Seidi, F. The Fe_3O_4@apple Seed Starch Core-Shell Structure Decorated In(III): A Green Biocatalyst for the One-Pot Multicomponent Synthesis of Pyrazole-Fused Isocoumarins Derivatives under Solvent-Free Conditions. *Int. J. Biol. Macromol.* **2021**, *190*, 61–71. [CrossRef] [PubMed]
15. Zhang, Y.; Ma, Z.; Ruan, K.; Gu, J. Flexible $Ti_3C_2T_x$/(Aramid Nanofiber/PVA) Composite Films for Superior Electromagnetic Interference Shielding. *Research* **2022**, *2022*, 9780290. [CrossRef] [PubMed]
16. Seidi, F.; Zhao, W.; Xiao, H.; Jin, Y.; Reza Saeb, M.; Zhao, C. Radical Polymerization as a Versatile Tool for Surface Grafting of Thin Hydrogel Films. *Polym. Chem.* **2020**, *11*, 4355–4381. [CrossRef]
17. Melvin, G.J.H.; Zhu, Y.; Ni, Q.-Q. Nanomaterials: Electromagnetic Wave Energy Loss. In *Nanotechnology: Applications in Energy, Drug and Food*; Siddiquee, S., Melvin, G.J.H., Rahman, M.M., Eds.; Springer International Publishing: Cham, Switzerland, 2019; pp. 73–97, ISBN 978-3-319-99602-8.
18. Cao, D.; Zhou, W.; Li, Y.; Liang, C.; Li, J.; Liu, D.; Wang, Y.; Li, T.; Cao, G.; Zhou, J.; et al. Tailoring the Dielectric Properties and Thermal Conductivity of F-Cu/PVDF Composites with SiO2 Shell as an Interfacial Layer. *Polym. Plast. Technol. Mater.* **2022**, *61*, 400–414. [CrossRef]
19. Jiang, D.; Murugadoss, V.; Wang, Y.; Lin, J.; Ding, T.; Wang, Z.; Shao, Q.; Wang, C.; Liu, H.; Lu, N.; et al. Electromagnetic Interference Shielding Polymers And Nanocomposites—A Review. *Polym. Rev.* **2019**, *59*, 280–337. Available online: https://www.tandfonline.com/doi/full/10.1080/15583724.2018.1546737 (accessed on 30 June 2022). [CrossRef]

20. Ma, P.-C.; Siddiqui, N.A.; Marom, G.; Kim, J.-K. Dispersion and Functionalization of Carbon Nanotubes for Polymer-Based Nanocomposites: A Review. *Compos. Part. Appl. Sci. Manuf.* **2010**, *41*, 1345–1367. [CrossRef]
21. Sun, R.; Zhang, H.B.; Liu, J.; Xie, X.; Yang, R.; Li, Y.; Hong, S.; Yu, Z. Highly Conductive Transition Metal Carbide/Carbonitride(MXene)@polystyrene Nanocomposites Fabricated by Electrostatic Assembly for Highly Efficient Electromagnetic Interference Shielding. *Adv. Funct. Mater.* **2017**, *27*, 1702807. Available online: https://onlinelibrary.wiley.com/doi/full/10.1002/adfm.201702807 (accessed on 30 June 2022). [CrossRef]
22. Geetha, S.; Kumar, K.K.S.; Rao, C.R.K.; Vijayan, M.; Trivedi, D.C. EMI Shielding: Methods And Materials—A Review. *J. Appl. Polym. Sci.* **2009**, *112*, 2073–2086. Available online: https://onlinelibrary.wiley.com/doi/full/10.1002/app.29812 (accessed on 30 June 2022). [CrossRef]
23. Li, S.; Huang, A.; Chen, Y.-J.; Li, D.; Turng, L.-S. Highly Filled Biochar/Ultra-High Molecular Weight Polyethylene/Linear Low Density Polyethylene Composites for High-Performance Electromagnetic Interference Shielding. *Compos. Part. B Eng.* **2018**, *153*, 277–284. [CrossRef]
24. Abraham, J.; Arif, P.M.; Xavier, P.; Bose, S.; George, S.C.; Kalarikkal, N.; Thomas, S. Investigation Into Dielectric Behaviour And Electromagnetic Interference Shielding Effectiveness Of Conducting Styrene Butadiene Rubber Composites Containing Ionic Liquid Modified MWCNT. *Polymer* **2017**, *112*, 102–115. Available online: https://www.sciencedirect.com/science/article/pii/S0032386117301040 (accessed on 30 June 2022). [CrossRef]
25. Ganguly, S.; Ghosh, S.; Das, P.; Das, T.K.; Ghosh, S.K.; Das, N.C. Poly(N-Vinylpyrrolidone)-Stabilized Colloidal Graphene-Reinforced Poly(Ethylene-Co-Methyl Acrylate) To Mitigate Electromagnetic Radiation Pollution. *Polym. Bull.* **2020**, *77*, 2923–2943. Available online: https://link.springer.com/article/10.1007/s00289-019-02892-y (accessed on 30 June 2022).
26. Cheng, H.-C.; Chen, C.-R.; Hsu, S.; Cheng, K.-B. Electromagnetic Shielding Effectiveness and Conductivity of PTFE/Ag/MWCNT Conductive Fabrics Using the Screen Printing Method. *Sustainability* **2020**, *12*, 5899. [CrossRef]
27. Ebrahimi, I.; Gashti, M.P. Polypyrrole-MWCNT-Ag Composites for Electromagnetic Shielding: Comparison between Chemical Deposition and UV-Reduction Approaches. *J. Phys. Chem. Solids* **2018**, *118*, 80–87. [CrossRef]
28. Kwon, S.; Ma, R.; Kim, U.; Choi, H.R.; Baik, S. Flexible Electromagnetic Interference Shields Made of Silver Flakes, Carbon Nanotubes and Nitrile Butadiene Rubber. *Carbon* **2014**, *68*, 118–124. [CrossRef]
29. Joseph, N.; Janardhanan, C.; Sebastian, M.T. Electromagnetic Interference Shielding Properties of Butyl Rubber-Single Walled Carbon Nanotube Composites. *Compos. Sci. Technol.* **2014**, *101*, 139–144. [CrossRef]
30. Formela, K.; Marć, M.; Wang, S.; Saeb, M.R. Interrelationship between Total Volatile Organic Compounds Emissions, Structure and Properties of Natural Rubber/Polycaprolactone Bio-Blends Cross-Linked with Peroxides. *Polym. Test.* **2017**, *60*, 405–412. [CrossRef]
31. Formela, K.; Hejna, A.; Piszczyk, Ł.; Saeb, M.R.; Colom, X. Processing And Structure–Property Relationships Of Natural Rubber/Wheat Bran Biocomposites. *Cellulose* **2016**, *23*, 3157–3175. Available online: https://link.springer.com/article/10.1007/s10570-016-1020-0 (accessed on 30 June 2022). [CrossRef]
32. Hema, S.; Sambhudevan, S.; Mahitha, P.M.; Sneha, K.; Advaith, P.S.; Rashid Sultan, K.; Sajith, M.; Jose, B.; Menon, S.K.; Shankar, B. Effect of Conducting Fillers in Natural Rubber Nanocomposites as Effective EMI Shielding Materials. *Mater. Today Proc.* **2020**, *25*, 274–277. [CrossRef]
33. Zhan, Y.; Oliviero, M.; Wang, J.; Sorrentino, A.; Buonocore, G.G.; Sorrentino, L.; Lavorgna, M.; Xia, H.; Iannace, S. Enhancing the EMI Shielding of Natural Rubber-Based Supercritical CO_2 Foams by Exploiting Their Porous Morphology and CNT Segregated Networks. *Nanoscale* **2019**, *11*, 1011–1020. [CrossRef]
34. ACS Symposium Series (ACS Publications). Available online: https://pubs.acs.org/doi/abs/10.1021/bk-2021-1380.ch009 (accessed on 30 June 2022).
35. Jose Varghese, R.; Vidya, L.; Joseph, T.M.; Gudimalla, A.; Harini Bhuvaneswari, G.; Thomas, S. Potential Applications of XLPE Nanocomposites in the Field of Cable Insulation. In *Crosslinkable Polyethylene Based Blends and Nanocomposites*; Springer: Berlin, Germany, 2021; pp. 197–213.
36. Perspectives of Cashew Nut Shell Liquid (CNSL) in a Pharmacotherapeuti. Available online: https://www.taylorfrancis.com/chapters/edit/10.1201/9781003057451-7/perspectives-cashew-nut-shell-liquid-cnsl-pharmacotherapeutic-context-tomy-muringayil-joseph-debarshi-kar-mahapatra-mereena-luke-j%C3%B3zef-haponiuk-sabu-thomas (accessed on 30 June 2022).
37. KI, S.; Nutenki, R.; Joseph, T.M.; Murali, S. Structural, Molecular and Thermal Properties of Cardanol Based Monomers and Polymers Synthesized via Atom Transfer Radical Polymerization (ATRP). *J. Macromol. Sci. Part. A* **2022**, *59*, 403–410. [CrossRef]
38. Muringayil Joseph, T.; Murali Nair, S.; Kattimuttathu Ittara, S.; Haponiuk, J.T.; Thomas, S. Copolymerization of Styrene and Pentadecylphenylmethacrylate (PDPMA): Synthesis, Characterization, Thermomechanical and Adhesion Properties. *Polymers* **2020**, *12*, 97. [CrossRef] [PubMed]
39. Tanaka, T.; Montanari, G.C.; Mulhaupt, R. Polymer Nanocomposites as Dielectrics and Electrical Insulation-Perspectives for Processing Technologies, Material Characterization and Future Applications. *IEEE Trans. Dielectr. Electr. Insul.* **2004**, *11*, 763–784. [CrossRef]
40. Zhang, H.; Hackam, R. Influence of Fog Parameters on the Aging of HTV Silicone Rubber. *IEEE Trans. Dielectr. Electr. Insul.* **1999**, *6*, 835–844. [CrossRef]
41. Kumar, R.; Palanivelu, K. Vulcanization, Mechanical and Dielectric Properties of Carbon Black/Nanoclay Reinforced Natural Rubber Hybrid Composites. *Appl. Mech. Mater.* **2015**, *766–767*, 377–382. [CrossRef]